

The Microchannel Plate Detector Electronics System for SPEAR

Ukwon Nam^a, Jingeun Rhee^{a,b}, Eric J. Korpela^d, Ho Jin^a, Daehee Lee^c,
Jeffery S. Hull^d, Peter Berg^d, Wonyong Han^a, Kyungwook Min^b, Jerry Edelstein^d

^aKorea Astronomy Observatory
61-1, Hwaam-dong, Yusong-gu
Taejon 305-348, Korea

^bSatellite Technology Research Center
Korea Advanced Institute of Science and Technology
373-1 Kusong-dong, Yusong-gu
Taejon 305-701, Korea

^cSpace Science Laboratory
University of California,
Berkeley, CA 94720-7450

ABSTRACT

The SPEAR (Spectroscopy of Plasma Evolution from Astrophysical Radiation) mission to map the far ultraviolet sky uses micro-channel plate (MCP) detectors with a crossed delay line anode to record photon arrival events. SPEAR has two MCP detectors, each with a ~25mm x 25 mm active area. The unconventional anode design allows for the use of a single set of position encoding electronics for both detector fields. The centroid position of the charge cloud, generated by the photon-stimulated MCP, is determined by measuring the arrival times at both ends of the anode following amplification and external delay. The temporal response of the detector electronics system determines the readout's positional resolution for the charge centroid. High temporal resolution (< 35ps x 75ps FWHM) and low power consumption (<6W) are required for the SPEAR detector electronics system. We describe the development and performance of the detector electronics system for the SPEAR mission.

Keywords : delay line anode, readout electronics, microchannel plate, far-ultraviolet

1. INTRODUCTION

The SPEAR (Spectroscopy of Plasma Evolution from Astrophysical Radiation) is a pathfinder mission to produce a full sky FUV (Far Ultra-Violet) emission spectrum¹. The instrument is aboard the Korean mini-satellite, KAISTSAT-4, provided by the Satellite Technology Research Center (SatRec). This satellite is to be launched mid 2003 on COSMOS, as secondary payload. The orbit is circular and sun synchronous at 800 km altitude.

SPEAR employs a dual channel, imaging spectrograph. One channel is optimized for O_{VI} region ($\lambda\lambda$ 900 – 1175 Å), and the other for the C_{IV} region ($\lambda\lambda$ 1335 – 1750 Å). The FUV photons from each optical channel are focused on the microchannel plate (MCP) detector placed at the focal plane. MCP detectors are established in extreme- and far-UV astronomy, and have flown on various missions including EUVE², IMAGE³, SOHO⁴, FUSE⁵. SPEAR employs MCP based crossed delay line (XDL) detector to record the photon arrival events. This type of detector generally consists of MCP stack, anode, and readout electronics. The MCP stack is an electron multiplier, which generates 10⁵ – 10⁷ electrons for each photon. The crossed delay line (XDL) anode consists of orthogonal set of charge gathering fingers which collect the charge generated by the MCP, and an external delay for each finger. Each detector has 25mm x 25mm active area format with 4096x1024 electronic resolution elements in each spectral (X) and imaging (Y) direction. The SPEAR position encoding method uses an anode that shares the delay lines in the spectral direction. This unconventional design

enables both spectral and image channels to share the anode and readout electronics. The spatial resolution requirement for the detector derived from science goals is $\sim 86\mu\text{m}$ in X and $\sim 100\mu\text{m}$ in Y.

We present the design of SPEAR detector system, primarily on the readout electronics, and test results from the detector system and electronics.

2. SYSTEM DESIGN

2.1. Overview

A microchannel plate based crossed delay line (XDL) detector is generally composed of MCP stack, anode, and readout electronics. The detector design of SPEAR is shown in fig.(1), (2). Two separate MCP stacks are used as detector for each optical channel. The 'Z' stacked MCPs are mounted in a brazed ceramic body, and clamped by the circumferential springs. This stacked body is attached to a plate that clamps the anode. The spacing between MCP bottom plate and the anode is set to be $\sim 7\text{mm}$. The MCP's have $12\mu\text{m}$ pores with $15\mu\text{m}$ spacing and 13° bias angle. They have circular format with 36mm diameter, and the diameter of active area is 33mm . The resistance of each plate is $\sim 200\text{M}\Omega$, and aspect ratio (length to diameter ratio) is 80:1. The XDL anode consists of two sets of orthogonal charge gathering fingers and external delay lines, which are connected to each finger. External



fig.(1) 3-D drawing of detector assembly

delay lines are constructed as a serpentine stripline on an alumina substrate ($\epsilon \sim 9.6$). Along the spectral (X) direction, the fingers in the short and long waveband share the external delay. The external delays in the image (Y) direction, are physically separated, but electrically connected to form single delay. This unconventional design of anode enables us to conserve power, weight, and volume, by using single set of readout electronics for both short and long waveband MCP detectors.

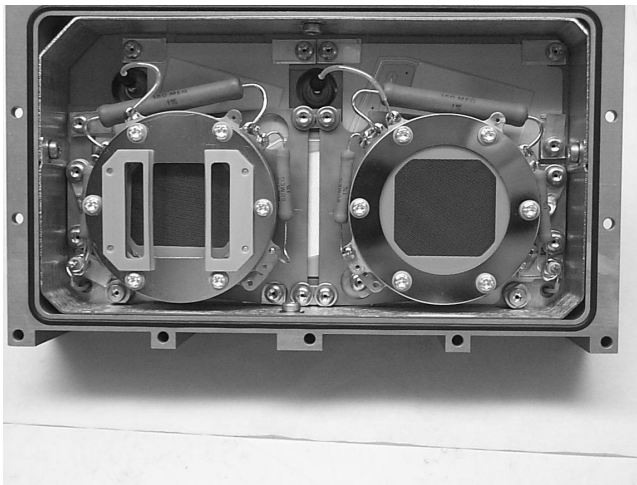


fig.(2) Photograph of flight SPEAR detector showing short and long waveband configurations

FUV photons focused at the MCP generate an electron cloud, which lands on the fingers of anode. This charge is nearly equally divided into the X and Y fingers, and propagates to the both ends of each delay line [fig(3)]. These signals are processed by the readout electronics consisting of fast amplifiers, a reference stimulator, and a time to digital converter (TDC). The event centroid position is deduced from the pulse arrival time differences between the two ends of each serpentine delay line. The X and Y event positions with event amplitude are digitized in the TDC. The electronic resolutions are 14 bit for X and Y, 8 bit for amplitude. These data are packetized into a 32bit format before telemetry to the ground.

2.2. Anode

To achieve required resolution, XDL anode and readouts are selected for SPEAR. In this scheme, two sets of orthogonal fingers cover the active area under the MCP. These fingers are attached to the external delay placed outside the active area [fig(4)].

The anode is ~120mm long x 70mm wide and is .015” inch thick; the substrate material is alumina with a dielectric constant of ~9.6. The anode is fabricated using standard silkscreen methods and materials. Care must be exercised in the fabrication of the raised Y fingers however. The raised fingers cross over, and are orthogonal to, the X fingers. The raised fingers intercept ~50% of the charge cloud and deliver it to the Y stripline and must be electrically isolated from the X stripline to preclude cross talk. The raised fingers are a multi-layer construction. The first layer is an insulator; the next layer is metallic and is grounded to electrically isolate the two striplines. The third layer is an insulator and the top layer is again metallic to bring the charge signal to the Y stripline. Tight tolerances and careful fabrication insure that the charge split is correct and that there are no shorts or opens. The delay line of X is shared by both the short and long waveband fingers, and the delay line of Y is physically separated for each waveband, but electrically connected to form a single delay. Delay time for X is ~32ns, and ~13ns delays for each waveband comprise total of ~27ns delays for Y. The anode fingers are rotated by 15° with respect to optical axis, to

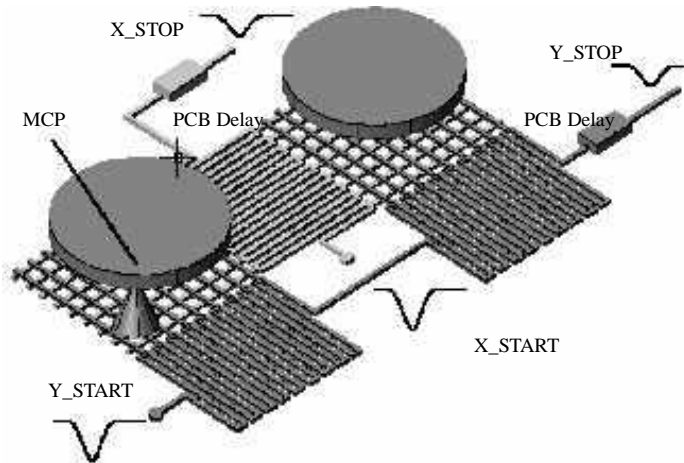


fig.(3) Schematic of operational configuration of the XDL detector

prevent any non-linearity in the anode and electronics from mimicking a spectral feature. The measured scale factor of the anode is ~0.44 $\mu\text{m}/\text{ps}$, and ~1.3 $\mu\text{m}/\text{ps}$ for each X and Y direction.

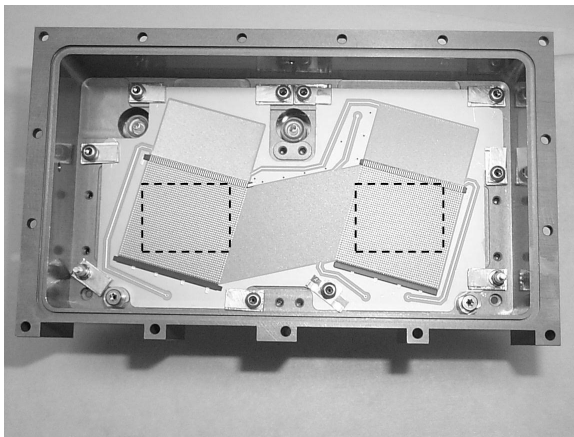
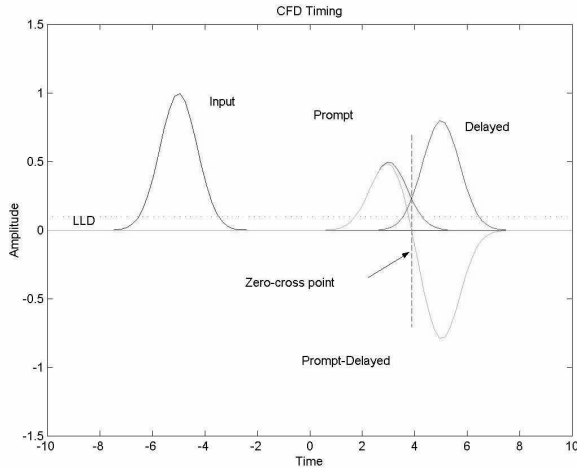


fig.(4) Photograph of flight SPEAR anode. The dashed rectangle shows the optical axis

regardless of the event position for proper processing. To do this, we put a PCB type transmission lines with a ~50ns delay as an extra delay at the “stop” end. A ~7.5m long stripline was constructed on a substrate of FR-4($\epsilon\sim 4.2$), to give rise to ~50ns of delay. It is possible use substrate of high dielectric constant to make the PCB more compact with the same delay. However, in that case, the signal suffers more attenuation and dispersion, which can degrade the pulse amplitude and shape. There is compromise between the compactness and pulse characteristics. The characteristic impedance of the fabricated PCB delay is ~45 Ω and DC resistance is ~4 Ω . Attenuation is measured to be ~3dB, and no appreciable change of pulse shape between the input and output is observed. A stimulator injects an artificial event signal into the amplifier at a fixed rate (~40Hz) so that thermal drifts in the position encoding system can be calibrated in flight. The TDC comprises three main sections: constant fraction discriminator (CFD), time to amplitude converter (TAC), and analog to digital converter (ADC), and their associated control and interface circuitry. The CFD is the most critical part in the readout electronics. It generates the logic pulses to start and stop the operation of TAC. The SPEAR CFD is constructed based on that presented by Lampton⁹. In this design, the crossing between the prompt and delayed pulses can be adjusted to occur at certain fraction of delayed pulse by selecting the delay taps for the two pulses. We

2.3. Readout electronics

The delay line readout electronics plays the role of recording the arrival time differences between the “start” and the “stop” signals from the XDL anode, and converting it to the digitized position which is directly related to this time difference. As displayed in the fig(6), it consists of fast amplifiers, stimulators, and time to digital converters (TDC) for each of the spectral (X) and imaging (Y) direction. The anode outputs are connected to the amplifiers using coaxial cables. For each channel, this high speed amplifier generates fast (~5ns FWHM) timing signals for the “start” and the “stop” output of the anode, and a slow (~1us) bipolar shaped pulses with peak voltage proportional to the input charge. The “stop” signal must arrive after the “start” signal



employed high speed CMOS comparators (MAX9686), and ACMOS gates (54ACT74) instead of ECL to reduce the power consumption. The TAC generates a voltage whose amplitude is proportional to the time difference between the two logic pulses created by the CFD. A constant current source is turned on during the time interval between the “start” and the “stop”. This current is integrated by the high quality capacitors to give rise to a voltage proportional to the time difference. A 14 bit ADC (AD679) is used to digitize the event positions. They are truncated to 12 bit (X), and 10 bit (Y) format to match the specification of the telemeter system.

fig.(5) Simulated pulses in the CFD showing the prompt and delayed pulse shapes and cross timing

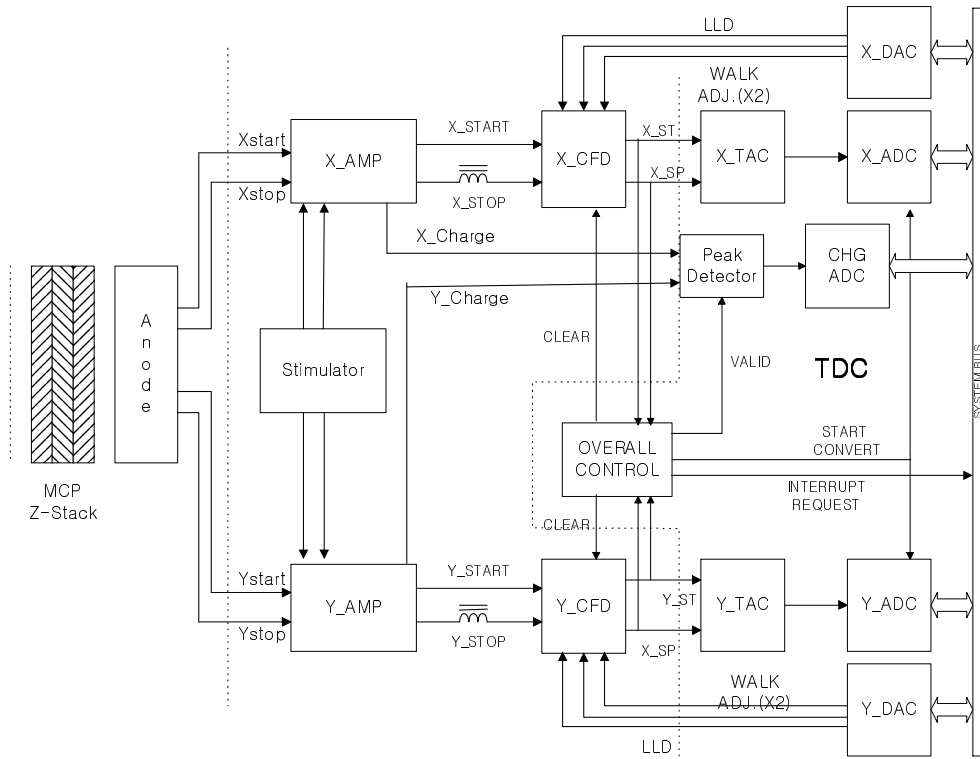


fig.(6) Block diagram of SPEAR readout electronics

3. TEST DATA

3.1. Electronics

A series of tests for the QM electronics were performed using bench pulser (Stanford Research : DG535), switchable delay, and stimulator. At first, TAC range was set using the simulator. The position of two stimulator pulses defines the two extreme ends of TDC. Digital position of the stimulator is set at ~1,000 and ~14,500 pixels, considering ~10%

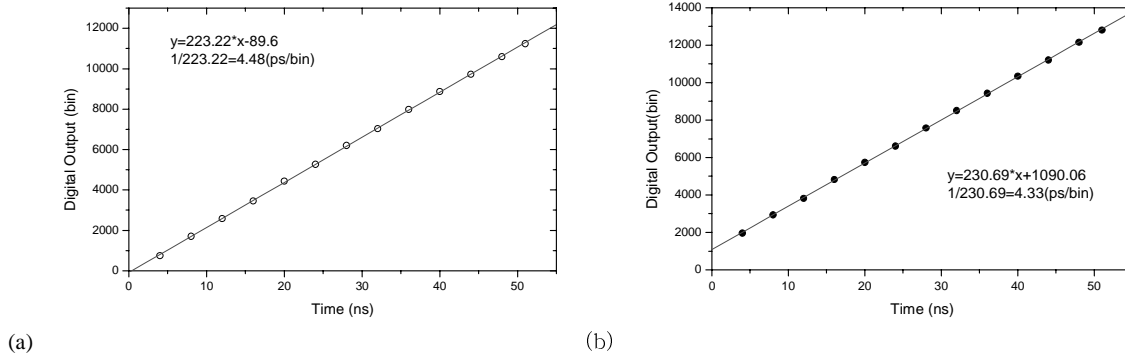


fig.(7) TAC linearity measurement results. (a) Y direction (b) X direction

margin for the stimulator position drift. After setting the TAC range, the linearity and bin size of TDC were measured using switchable delay. The measured bin size of each X and Y TDC are ~4.3 ps and ~4.5ps [fig(7)]. The resolution

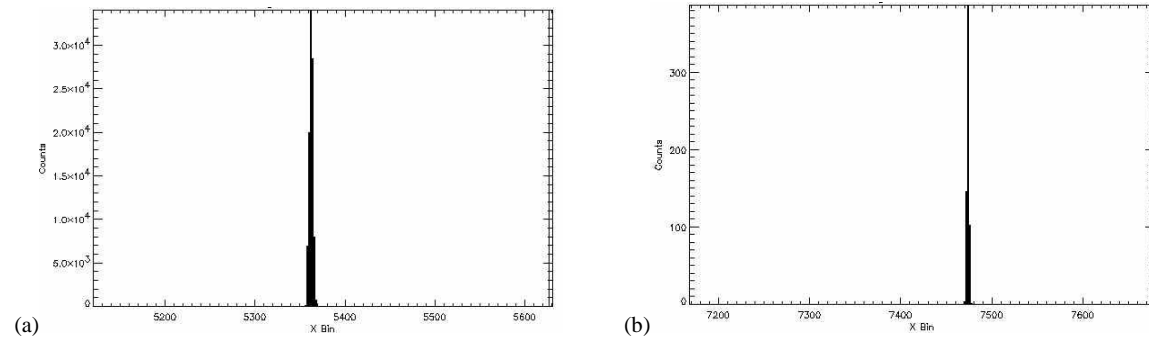


fig.(8) Distribution of events generated by the bench pulser and stimulator. (a) bench pulser (b) stimulator

performance of TDC was tested using the bench pulser and appropriate pulse shaper. The result in fig(8) shows ~40ps of the FWHM temporal resolution. The limiting electronic resolution including amplifier and anode can be determined by the stimulator. The results in fig(9) shows ~40ps FWHM temporal resolution. Considering the scale factor of SPEAR anode, this corresponds to ~20 μ m, and ~50 μ m spatial resolution. The two results were nearly the same, and this implies

that the TDC is the dominant contributor of electronic resolution. We also tested the walk effect by changing the output amplitude of the stimulator. The result displayed in fig(9) shows that over 1/30 of the input amplitude peak position moves ~50ps (~22 μ m). The major factors that can affect the resolution performance of the delay line electronics includes pulse shape, amplifier noise, walk and jitter in the CFD, TAC noise, and ADC bin errors. Among these TAC and ADC contributions are residual, and can be corrected later. For this purpose, we performed DNL

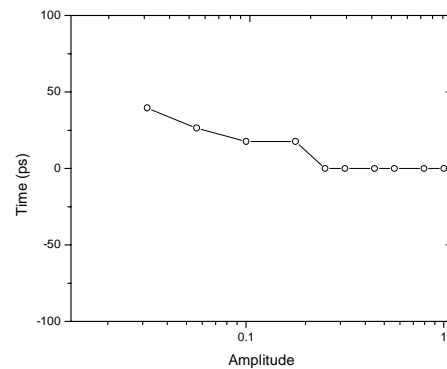


fig.(9) The result of walk test with stimulator

measurements using random pulser. Other than the factors listed above, temperature stability, rate immunity, and power supply rejection characteristics can also affect the performance, and we tested these characteristics during the basic function test period.

3.2. Image

To evaluate the resolution with photons, we used pinhole mask with 10 μ m holes and 1 mm center spacing. Image of pinholes near the center, and cross section histogram of X and Y direction is also displayed in fig(10). Optimization of the electronics is still in progress, and this image was taken during the optimization process. The currently measured average spatial resolution of the detector system was $\sim 80\mu\text{m}$ (X) and $\sim 110\mu\text{m}$ (Y). This level of performance barely requirements derived from the science goals.

Quick shot of flat field image was also taken with the flight detector as a reference data for the vibration test, shown in fig(11). Dead spots due to the MCP fabrication defects are shown in this image. X and Y histogram shows the variation in the image intensity.

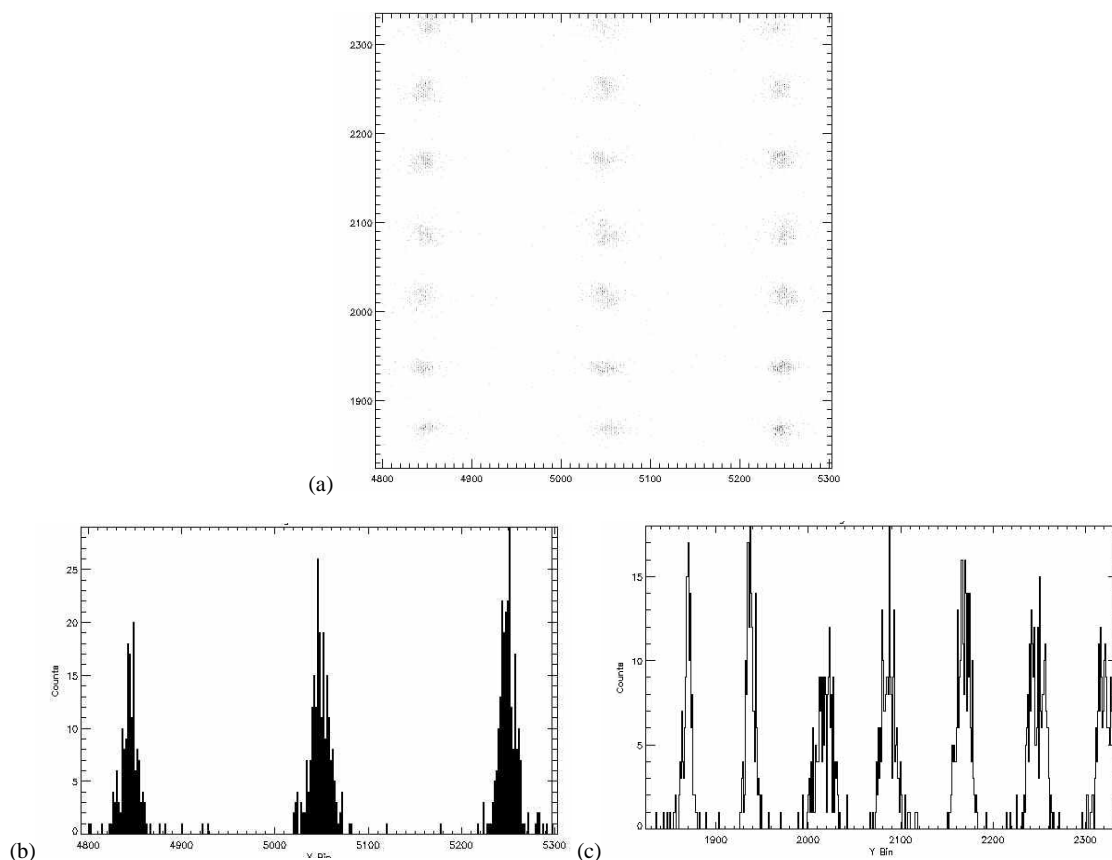
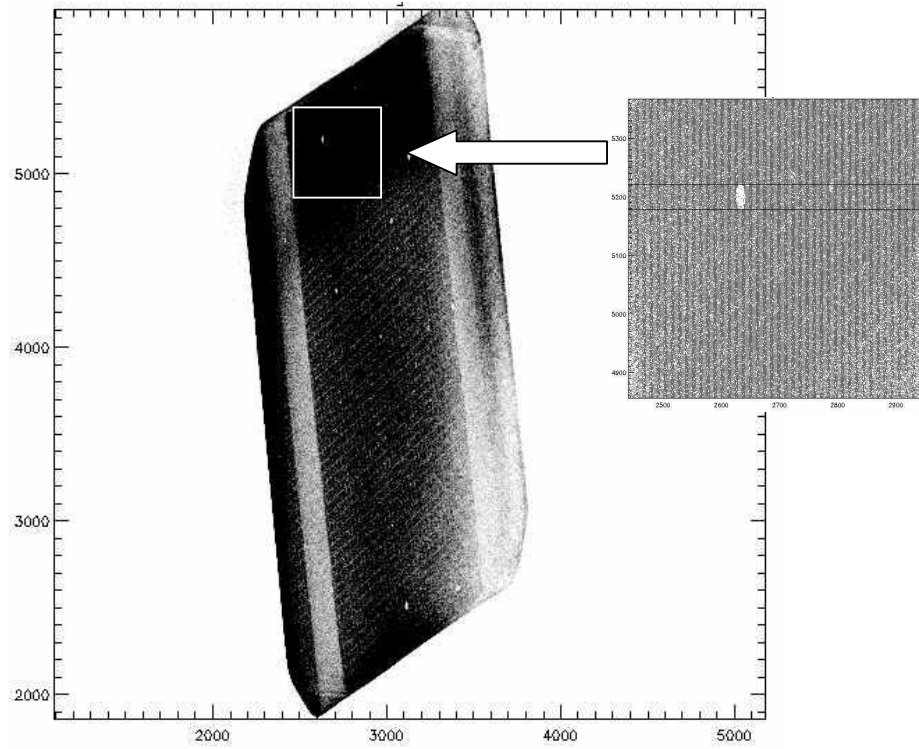


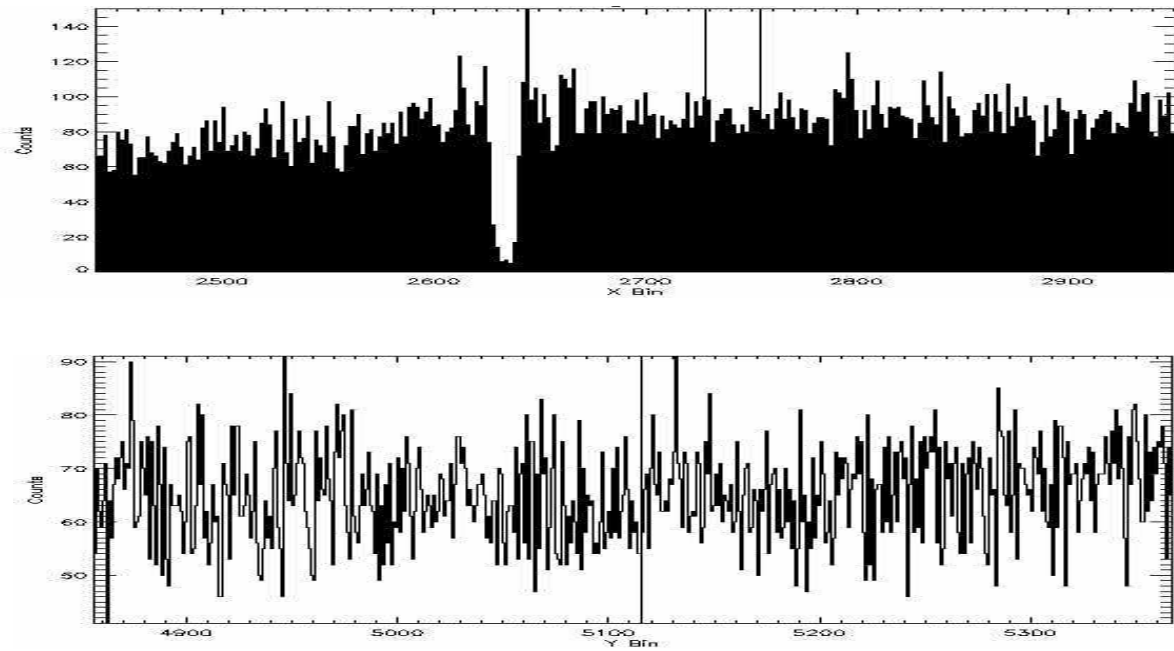
fig.(10) Pinhole image and corresponding histograms near the center for X and Y direction. (a) pinhole image near the center (b) X cross sectional histogram (c) Y cross sectional histogram

4. CONCLUSION

We have constructed and are testing MCP based XDL detector system for SPEAR. The anode and readout electronics are designed to fit the purpose of the SPEAR. The resolution test of the SPEAR electronics is performed using reference pulser and stimulator. The limit of the spatial resolution we can get with current electronics is measured to be $\sim 20\mu\text{m}$



fig(11) Flat field image of the short waveband detector.



fig(12) X and Y histogram of zoomed area in fig(11).

FWHM (X) and $\sim 50\mu\text{m}$ FWHM (Y). We are testing the detector system with photons, and primary results we got are $\sim 80\mu\text{m}$ (X) and $\sim 110\mu\text{m}$ (Y). This can be improved during the optimization process, to meet the performance requirement.

ACKNOWLEDGEMENTS

We would like to thank John Vallerga, and Rick Raffantii for their valuable comments and we also thank Mike Lampton, and David Stone. Many grateful thanks are extended to the many unmentioned people who contributed to SPEAR project.

REFERENCES

1. J. Edelstein et. al., *this vol*, (2002)
2. O. H. W. Siegmund, R. F. Malina, K. Coburn, and D. Werthimer, *IEEE Trans. Nucl. Sci.*, **NS-31**, 776 (1984)
3. J. M. Stock, O. H. W. Siegmund, J. S. Hull, K. E. Kromer, S. R. Jelinsky, H. D. Heetderts, M. Lampton, and S. B. Mende, *Proc. SPIE*, **3445**, 407 (1998)
4. O. H. W. Siegmund, M. A. Gummin, T. Sasseen, P. N. Jelinsky, G. A. Gaines, J. Hull, J. M. Stock, M. L. Edgar, B. Y. Welsh, S. R. Jelinsky, and J. V. Vallerga, *Proc. SPIE*, **2518**, 344 (1995)
5. O. H. W. Siegmund, M. Gummin, J. Stock, G. Naletto, G. Gaines, R. Raffanti, J. Hull, R. Abiad, T. Rodriguez-Bell, T. Magoncelli, P. Jellinsky, W. Donakowski, and K. Kromer, *Proc. SPIE*, 3114, (1997)
6. M. Lampton, *Rev. Sci. Instrum.*, **69**, (1998)

* uwnam@kao.re.kr; phone 82 42 865 3221; fax 82 42 861 5610; <http://www.kao.re.kr>; Korea Astronomy Observatory, Hwam Dong, Yusong Gu, Taejon, Korea,

**jrhee@space.kaist.ac.kr; phone 82 42 869 2565; fax 82 42 861 5610; <http://space.kaist.ac.kr>; Korea Advanced Institute of Science and Technology,